REPEATABILITY OF ADHESION FORCE MEASUREMENT ON WOOD LONGITUDINAL CUT CELL WALL USING ATOMIC FORCE MICROSCOPY[1]

*Juan Li**

Ph.D. candidate
Organic and Wood Based Materials
Institute of Building Materials, Concrete Construction and Fire Safety
Department of Civil and Environmental Engineering, TU Braunschweig
Braunschweig 38102, Germany
E-mail: juan.li@tu-braunschweig.de

Kasal Bohumil

Professor
Organic and Wood Based Materials
Institute of Building Materials, Concrete Construction and Fire Safety
TU Braunschweig
Braunschweig 38102, Germany
Fraunhofer Wilhelm-Klauditz-Institut WKI
Braunschweig 38108, Germany
E-mail: bohumil.kasal@wki.fraunhofer.de

(Received May 2020)

Abstract. As a powerful tool to investigate the surface properties at a nanoscale resolution, the atomic force microscopy (AFM) encounters challenges in the measurement of plant materials such as wood surface. In particular, for rough and heterogeneous surfaces, a robust and easily performed positioning method is necessary for reproducible measurements. One of the critical issues is the ability to position the AFM tip after the specimens are removed for treatments from a device and repeatedly analyzed. If the tip is not repeatably positioned within the measured area, the natural variability of the surface (such as surface roughness) can mask the effects of treatments of interest. In this article, a positioning method using the bordered pit of the wood radial surface as a natural marker is proposed and a systematic measurement procedure is presented. The idea results from the uniqueness of the anatomical features of a natural material (wood in this case) and the low probability of having exactly the same geometry of pit clusters in the vicinity of the area of interest. The results show that the anatomical features can be used as unique markers for precise positioning of the AFM tip. The process is demonstrated using an example of the effect of temperature on adhesion forces on the wood surface. After the heat treatment, the wood surface layers were investigated with Fourier transform infrared spectroscopy and attenuated total reflection (FTIR-ATR).

Keywords: AFM, cell wall, pit, adhesion force, repeatability.

INTRODUCTION

Reliable methods of the nanoscale characterization of wood material are required to study the surface properties and effects of the environment on the surface. Atomic force microscopy (AFM) provides a nanometer resolution of imaging, mechanical, electrical, magnetic, and thermal characterization of different materials in their natural state (Robertson et al 1996; Nowicki et al 2003; Nguyen et al 2011; Revilla et al 2012). Whereas synthetic surfaces or metal surfaces can be prepared with a high level of consistency and repeatability, preparing a smooth homogeneous surface of the wood at a nano- or even microlevel is impossible, and inherent surface roughness cannot be overcome.

The repositioning of the sample during AFM measurements has been a common concern for material characterization before and after exposure, especially for heterogeneous materials that

* Corresponding author

need to be removed from the device. Finding the precise location of the original measurement is critical in materials with high variability of surface properties, especially when comparative measurements are to be performed. Mechanical markers such as nanoscratches and microhardness indents have been reported to be used as reference points (RPs) for positioning during AFM measurements (Proff et al 2010; Sikora 2013, 2014). Abu Quba et al (2020) gave a thorough review of the relocation methods for AFM measurements on heterogeneous natural samples by different researchers, such as alpha-numeric relocation labels on mica surfaces (Wu et al 2002), a grid guide relocation setup (Markiewicz and Goh 1997), a grid in the backside of a mica sheet (Liu et al 2005), and other works in a fluid environment (O'Hagan et al 2004; Su et al 2004; Kao et al 2016; Janel et al 2017). The specific advantages and limits of different working principles were discussed. For example, artificial markers might damage the sample surface and disappeared after treatments on samples; some methods required a transparent sample to find the markers on the backside; some markers required time-consuming procedures to be created. The same author proposed to fix particles and cells on a semitransparent resin embedded with TEM grids, and this method allowed for repeated identification of the scanned area with high accuracy.

The literature sees few applications of AFM on wood material because of the heterogeneity of the wood surface. Wood surfaces are soft and uneven with concave lumens, pit cavities, overhanging cell walls (CWs), and debris which are challenging for the repeatability of measurements by AFM. A cross-hair drawn by a sharp pen on a wood surface was tried for positioning of the measurement area before and after solar radiation exposure (Meincken and Evans 2009), but no details about the positioning method were given in this article. Micro- or nanoscale positioning using a macro pen marker proved to be difficult. Also, a pen marker had the disadvantage of being removed or altered during treatment conditions. Later, the authors suggested spin-coated lignin and cellulose films as material models for wood exposed to solar radiation (Meincken and Evans 2009) because smoother and more homogeneous surfaces were much easier for AFM measurements. Artificially produced films however were no longer the true representation of the wood surface. Wood lumen surface and freshly cut CWs were observed to have different adhesion forces because of the chemical heterogeneity (Frybort et al 2014). Different locations on the wood CW were measured, and it was suggested that the variability of the adhesion force distribution was mainly induced by the variation of surface roughness of the wood CW (Jin and Kasal 2016). Topographic and phase-contrast images on the wood surface were measured before and after plasma treatment, and the images provided information about the changes of wood composites on CW layers (Acda et al 2011). Arnould and Arinero (2015) used the contact resonance mode of the AFM to obtain viscoelastic properties of the wood CW that was embedded in a resin. Casdorff et al (2017) reported the quantitative imaging QI™ (NanoWizard 4, JPK Instruments AG, Billerica, Massachusetts, United States) mode in the AFM which allowed for distinguishing CW layers of the compound middle lamella, S1, and S2 based on their Young's moduli. However, no systematic description of the positioning method and statistical analysis regarding the variation of measurements were given in the literature.

This study introduces a simple method that uses natural anatomical features of wood as markers, thus avoiding time-consuming artificial marking. A robust relocating method is critical when a material is subjected to treatments for which the samples must be removed from the AFM device. The ability to scan the identical area before and after treatment(s) is necessary to establish the effects of the treatments without contamination of the data attributable to spatial variability of the surface. In this study, the unique arrangements of pits were used as natural markers on the wood surface and acted as the RP for AFM measurements. This method consists of two steps: initial identification of pit clusters on the wood radial surface and precise identification of CW location using a certain pit in a chosen pit cluster. This

permitted considering defined clusters as unique and optically recognizable fiducial markers. As the natural irregularities in softwood tracheid CWs, bordered pits were the observable natural openings with associated borders (Sirviö and Kärenlampi 1998). In earlywood, the number of pits varies from 50 to 300 per tracheid (Stamm 1970). The diameter of bordered pits was reported to be less than 20 μm in earlywood and ca. 50% of tracheid width (Koran 1977). The pit aperture diameter was in the range of 5-7 μm (Domec et al 2006). Pit dimensions are in the horizontal measurement range of AFM.

An easily recognizable pit was chosen as the natural marker on the wood surface and acted as the RP for AFM measurements. The pit and its vicinity were digitally stored as a unique cluster that could be repeatedly located. The same pit was repositioned with the built-in camera (model: N9451A, Agilent Technologies 5500; Agilent Technologies, Inc., Santa Clara, CA) in the AFM during each measurement. A method was developed to use a chosen pit and the pit aperture to reposition the same section of the adjacent wood CW. This technique was further illustrated in a series of tests of the effect of temperature on the adhesion measurement on the wood surface. The results showed that this positioning method provided high repeatability of the measurement of adhesion forces on the radial surface of the wood CW. The presented results for the temperature–force relationship are used to demonstrate the robustness of the proposed relocation technique and it is not necessarily to make final statements about this relationship itself—this is a subject of ongoing work.

MATERIALS AND METHODS

The radial surface of spruce wood (*Picea abies*) with dimensions of approximately 3×4.5 mm was cut with a platinum-coated blade. The sample was stored in a desiccator (less than 15% RH, 21 ± 2°C) for at least 1 wk to allow the initial inactivation of the fresh surface and obtain a relatively stable state (Frybort et al 2014). The sample was mounted on a heating sample plate (range: room temperature to 250°C) and connected with a Lake Shore temperature controller 331 (Lake Shore Cryotronics, Inc., Westerville, OH) for precise temperature control (error: $\pm$ 0.5°C). The AFM (Agilent Technologies 5500; Agilent Technologies, Inc.) device was turned on for 3 h for stabilization, and the environmental chamber was flushed with N_2 for 1 h to dry the sample surface before measurement. During force measurement, the sample was kept in a dry atmosphere with a steady and slow flow of N_2, and the RH was continuously monitored to be less than 1%. Thus, the wood surface during measurement was assumed to be in a dry state, and the MC of the sample was approaching or being equal to 0%. After heat treatment, the wood sample was cut into surface layers for Fourier transform infrared spectroscopy (FTIR) measurements. A fresh sample without heat treatment was used for FTIR measurements as a control sample.

AFM Adhesion Force Measurement

Force measurement was conducted with a silicon Multi75Al-G tip with a reflex aluminum coating (BudgetSensors, rotated shape, nominal radius < 10 nm). The force constant (k) was determined with the thermal noise method to be 1.01 N/m. The laser alignment of the tip was kept the same, and the same tip was used during all measurements. During the force measurements, the deflection of the cantilever, x, and the position of the piezo, z, were recorded. The force F was calculated as multiplying the deflection of the cantilever by the force constant k: $F = k \times x$. One force–distance curve is shown in Fig 1. When the cantilever approaches the sample surface at a large separation distance at point a, there is no interaction between the tip and sample surface. As the cantilever continues to approach the sample, the tip is pulled down by the attraction force and snap-to-contact with the surface without a real load at point b. When the cantilever moves further toward the surface, it bends upward until a predefined load is reached. Then, at point c, the cantilever starts to retract from the surface. At point d, the tip stays in contact with the surface because of the adhesion force, and the cantilever bends downward until the maximum adhesion force is reached.

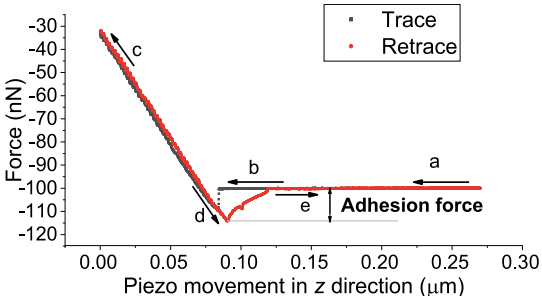

Figure 1. A force–distance curve between the atomic force microscopy tip and the wood surface. Point a: the cantilever approaches the sample surface at a large separation distance; point b: the cantilever snaps-to-contact with the surface; point c: the cantilever bends until a predefined load is reached and the retract curve starts; point d: the tip stays in contact with the surface and the cantilever bends downward until the maximum adhesion force is reached; the point e: the tip is separated from the surface.

Positioning Method

As the natural irregularities in the CW, pits were used as the recognizable feature for the position of the CW section in this study. As the first step, before measurements in the AFM, the radial surface of the wood sample was carefully examined in a light microscope. A schematic drawing of the wood radial surface with dimensions of m and n ($m = 3$ mm, $n = 6$ mm in this article) is shown in Fig 2, three clusters of pits labeled as a, b, and c have specific relative locations within a Cartesian coordinate system with an origin at the most left lower point. After the initial screening of the surface with the light microscope and the installed camera in the AFM, a rough mapping of the distributions of pit clusters could be determined. For example, the cluster with a loose pit distribution is located at the upper left corner, and the cluster b with a tight pit distribution is located in the middle part of the surface. For a sample with a small surface needed for AFM measurement, the coarse identification of pit clusters could be easily performed. After the coarse identification, a specific pit in one cluster was selected for further precise locating of the adjacent CW.

As shown in Fig 3, a cluster with a loose pit distribution in the earlywood was chosen for further measurements. In the second step, an easily recognizable pit was chosen to precisely locate its adjacent CW. In Fig 3, bordered pits are

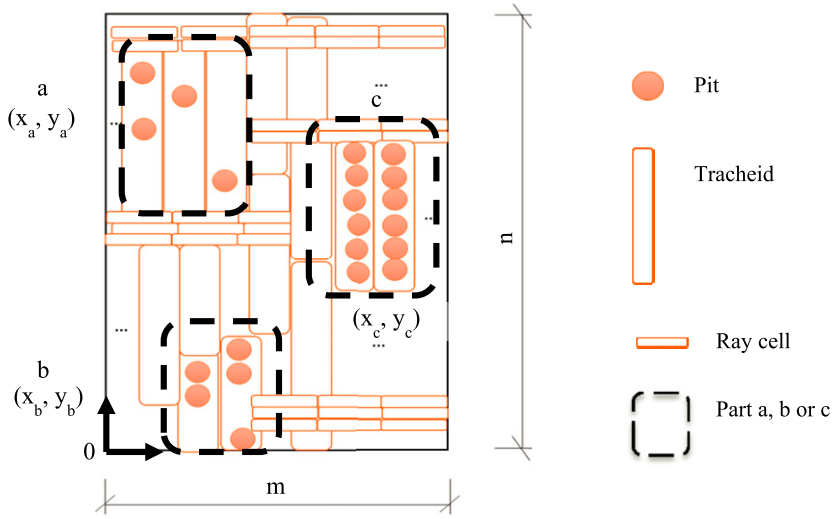

Figure 2. Coarse locating of a pit cluster on the wood radial surface. On a finely cut wood radial surface with dimensions of m and n, the origin of a Cartesian coordinate system is assumed to be somewhere, such as at the left down corner. There are different pit clusters such as a, b, and c in the figure. These clusters can be coarsely located using both, the digital camera in the atomic force microscopy and a light microscopy. A cluster can be chosen for further investigation. Within one cluster, a pit can be chosen to accurately locate the adjacent cell wall.

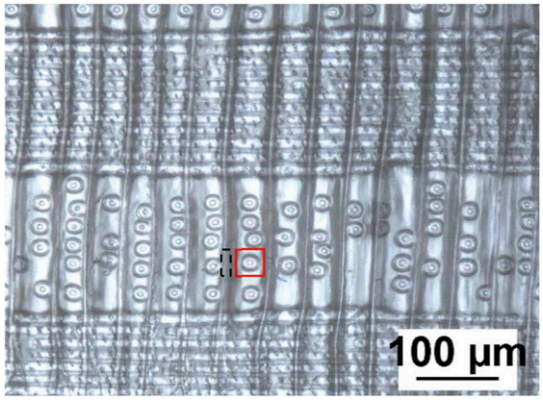

Figure 3. A cluster of pits and a chosen pit on the wood radial surface (Carl Zeiss, D-7082). A cell with coarse pits is easy to position, and a pit is chosen in the vicinity of the coarse area. For example, a pit in the red square was chosen as a target to position the adjacent cell left wall in the black square.

like chains of beads along the fiber direction. Under the light microscopy (Carl Zeiss, D-7082, Oberkochen, Germany), the lumen surface appears brighter than the pit area. Pits are distributed in a tight or loose manner with a bright lumen surface in between. The loose clusters of pits differentiate the wood cell from the surroundings. A pit in the vicinity was chosen as the recognizable feature for further positioning of the CW. The unique surrounding arrangement of pits and lumen surface helped with the identification of the pit. For repeated positioning with the AFM camera, the selected area was documented in detail, and several rounds of practice were suggested before removing the sample. This was a new procedure that was performed "manually", and images were compared by the operator because no computer algorithm exists to automate the procedure. The clusters however were relatively easy to be found and presented little difficulties.

The limited vertical measuring distance in the AFM is 6-8 µm (Meincken and Evans 2010), and the vertical roughness in the wood cell is typically less than 20 µm. The chosen CW, pit, and lumen surface were determined to have a height difference of less than 4 µm. In the AFM digital camera (N9451A), the chosen pit in light microscopy was positioned, and a 4-step procedure was used to position the CW section during each measurement.

The 4-step procedure is shown in Figs 4 and 5. The chosen pit and adjacent CW were imaged in the contact mode. The bottom of the pit aperture was chosen as the RP, and the tangent on the RP measuring d_0 intersected the adjacent CW in step 1 (Fig 4[a]). The intersection line was taken as the reference to position the zoomed scan area ($a \times a$) of the CW (Fig 4[a]). The scan area was extended four times in the longitudinal direction to obtain a measurement area with dimensions of $a \times 4a$ to minimize the positioning error in step 2 (Fig 4[b]).

The image in Fig 5(a) was measured in a scan range of 16 × 16 µm, with 256 pixels in each line. The zoomed measurement area was positioned with the tangent and determined to be 2 × 8 µm along the CW in Fig 6. The measurement time of force volume (FV) mode on this CW section was about 13 min. The natural concave or convex features on the CW were used for further precise positioning of the scanning area. The positioning error was determined to be ca. 0.2 µm along (e_1) and across (e_2) the fiber direction. Across the fiber direction, the scan area was set to always incorporate the entire CW, that is, the measurement width was always larger than the CW width. The relative positioning errors along and across the fiber direction were determined as follows:

$$\frac{e_1}{l} \approx \frac{0.2\ \mu\text{m}}{8\ \mu\text{m}} \tag{1}$$

$$\frac{e_2}{w} \approx \frac{0.2\ \mu\text{m}}{2\ \mu\text{m}} \tag{2}$$

The relative positioning errors could be neglected because the overlapping part of each measurement area was significantly larger than the part representing the nonoverlapping scan area. The FV mode in a 2D array with $8 \times 32 = 256$ pixels was used for the force measurements. A complete force–distance curve was measured in each pixel.

Repeatability of the Positioning Method

Relocating tests at room temperature. To show the repeatability of measurements using the proposed relocating method, adhesion force

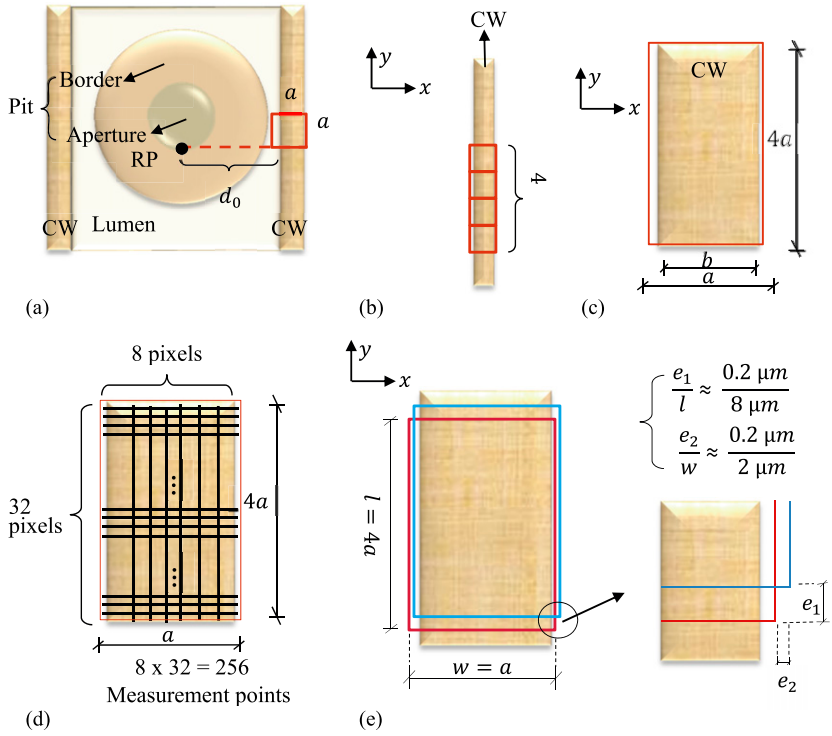

Figure 4. (a) Step 1: Imaging of the radial surface of wood cell wall (CW) in tapping mode by the atomic force microscopy (AFM) pit border, pit aperture, lumen surface, and CW. Positioning tool: reference point (RP), a tangent measuring $d_0$on the RP and zoomed scan area (red) with dimensions of $a \times a$. (b) Step 2: The scan area was extended to four times along the longitudinal direction of the cell wall (CW). (c) Step 3: The imaging of the CW section in the tapping mode by the AFM with dimensions of $a \times 4a$. The measurement width $a >$ the CW width b. (d) Step 4: Force measurements on the CW section in force–volume (FV) mode in a 2D array with $8 \times 32 = 256$ pixels. A force–distance curve was generated on each pixel in sequence. (e) e_1: position error in x direction (across the fiber); e_2: position error in y direction (along the fiber); w: the width of the measurement area; l: the length of the measurement area ($l = 4w$).

measurements on the wood CW were conducted on different days and at different temperatures to examine possible experimental errors. As shown in Table 1, at room temperature around 20°C, repositioning tests on the CW were conducted on three days, which were coded as D1, D2, and D3, and two, five and four measurements were performed, respectively. At the end of each testing day, the AFM device was turned off, and the sample holder plate was taken out and stored in a desiccator (RH less than 15%, 20 ± 3°C).

The error from the device drifting was also measured on the same positioned measurement area without lifting the tip. Five measurements were conducted. Between measurements, the sample was kept unmoved and the experimental condition was kept the same. The AFM tip stayed on the sample surface, started at the same point and moved in the same direction during each measurement. Each measurement was conducted in the FV mode with 256 measurement points.

Relocating tests at elevated temperature. The effect of the temperature on the adhesion forces was used to test the robustness of the repositioning procedures. Before heating, the tip was lifted at least 120 µm from the sample surface. After heating was turned on, the AFM scanner needed 20 min to stabilize. The measurement area

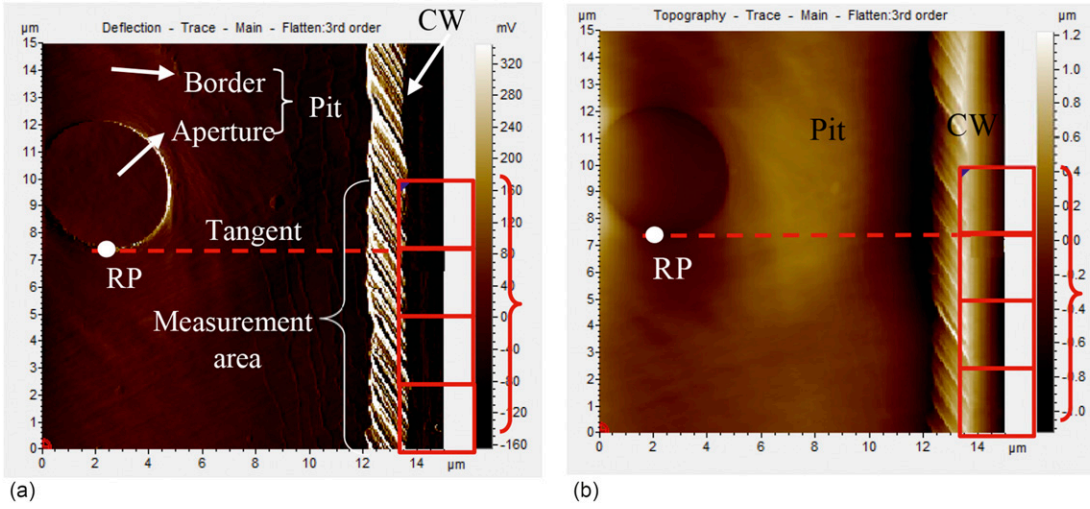

Figure 5. Deflection and topography images of the radial surface of the wood sample in the tapping mode by the atomic force microscopy (AFM) Pit border, pit aperture, and cell wall (CW) with a Multi75Al-G AFM tip (BudgetSensors, rotated shape, nominal radius < 10 nm). The zoomed scan area was positioned by the reference point (RP) on the bottom of the aperture. The lengthened measurement area with dimensions of 2×8 μm was determined for force–volume measurements.

on the CW was positioned with the method described earlier. The FV mode with 256 measurement points was applied.

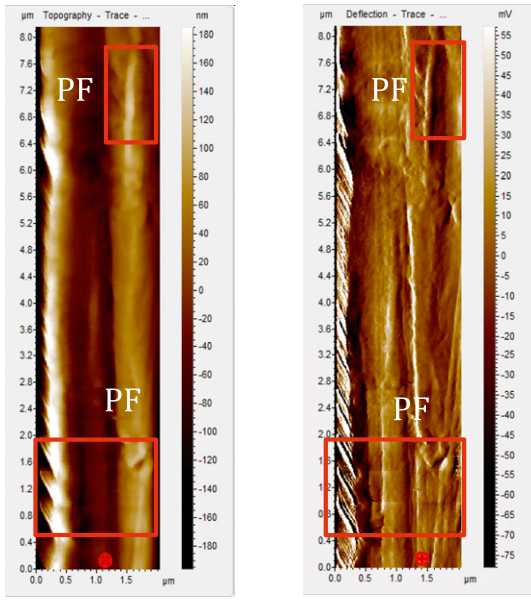

Figure 6. Deflection and topography images of the measurement area of the cell wall (CW). The scan area was 2×8 μm. The concave or convex area was taken as the positioning feature (PF) on the CW for precise positioning of measurement area with the *X* and *Y* offset on the scan controls panel.

As shown in Table 1 and Fig 7, the measurements at elevated temperatures were conducted within 2 d with coding D4 and D5. On day D4, the sample was heated to 60°C, and relocating measurements were carried out when the heating lasted for 40 and 70 min. The tests on day D4 were coded as D41 and D42. After the heating tests on day D4, the sample was stored in a desiccator (RH less than 15%, 20 ± 3°C) for 12 h to stabilize. Three relocating tests were conducted on the stabilized sample at room temperature around 20°C and coded as D43, D44, and D45. On day D5, the sample was heated at 90°C, and three relocating measurements during heating were conducted when the heating lasted for 40 min, 90 min, and 120 min. The tests on day D5 during heating were coded as D51, D52, and D53. After the sample was stored in a desiccator (RH less than 15%, 20 ± 3°C) for 12 h for cooling and stabilization, three relocating tests were performed at room temperature around 20°C and coded as D54, D55, and D56. In each of these tests, the relocating procedure described previously was used to eliminate the effects of spatial variations in the wood surface, which may mask the effects of the treatments.

Table 1. Design of relocating test on wood cell wall at different temperatures.

Day	No[a]	Temperature	Test notation[b]
D1	2	20°C	D11, D12
D2	5	20°C	D21, D22, D23, D24, D25,
D3	4	20°C	D31, D32, D33, D34
D4	2	60°C	D41, D42
	3	20°C	D43, D44, D45
D5	3	90°C	D51, D52, D53
	2	20°C	D54, D55, D56

[a] No.: number of relocating tests.
[b] Di_j: jth measurement on the day i according to the test sequence.

FTIR Investigation

As shown in Fig 8, after the repeating measurements with the AFM at room temperature and elevated temperature (a), the wood sample was cut with a blade into four surface layers in sequence (b) which were designated as L1, L2, L3, and L4 with the thickness of 0.23, 0.23, 0.16, and 0.20 mm, respectively (c). The four surface layers were measured with a Bruker Tensor 27 FTIR equipped with attenuated total reflection (Bruker Optics, Bremen, Germany). The spectra were collected in the wavenumber range of 4000-400 cm^{-1} at a resolution of 2 cm^{-1} with 32 scans. The spectra were baseline-corrected with OPUS software (OPUS 6.5, Bruker Optics, Bremen, Germany). Three measurements were performed on each surface layer, and the average was calculated as the representing spectrum. A maximum–minimum normalization was applied to all spectra. Surface layers from a fresh spruce wood sample were measured with FTIR as a comparison.

RESULTS AND DISCUSSION

Repeatability of the Positioning Method

To test the repositioning method, we first repeatedly relocated the scanning area without subjecting the specimen to any treatment. This was performed to test whether we were able to position the tip and conduct the identical scan even if the device was turned off, and the specimen was removed. We also conducted a series of experiments, in which the tip was repeatedly repositioned without moving the sample. This was carried out to test the repeatability of the device itself. This was important to separate the inherent measurement error from the errors due to the repositioning itself. The zero hypothesis was that both expected means and standard deviations were equal for all measurements. The assumption was that no significant changes to the surface and the tip occurred during and after the scanning.

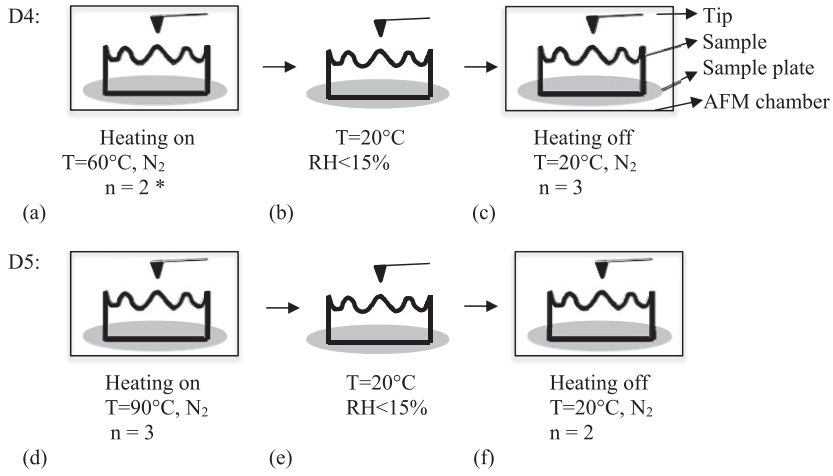

Figure 7. Relocating tests at elevated temperature. On day D4, (a) the sample was heated at 60°C, and two relocating tests were performed. The tests were labeled as D41 and D42. (b) Sample was taken out of the atomic force microscopy chamber and put in the desiccator for 12 h for stabilization. (c) Sample was tested at 20°C, and three relocating tests were conducted. The tests were labeled as D43, D44, and D45. On day D5, similar tests were repeated. * Number of relocating tests.

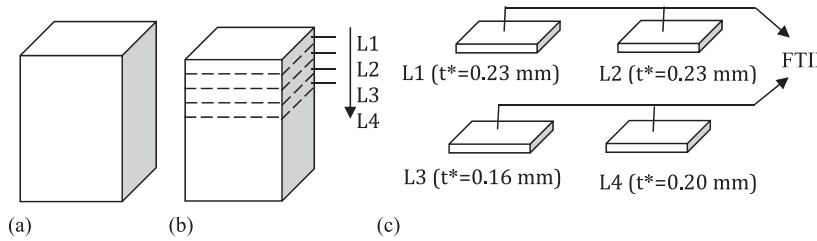

Figure 8. Fourier transform infrared spectroscopy (FTIR) measurements on the surface layers of the wood sample after the heat treatment. (a) Wood sample was used for relocating measurements with atomic force microscopy and measurements with heating; (b) after measurements and treatments in the procedure (a), the sample was cut with a blade into four surface layers (L1, L2, L3, and L4 in sequence); (c) Surface layers (L1, L2, L3, and L4) were measured by FTIR. The thicknesses (*t*) of L1, L2, L3, and L4 were 0.23, 0.23, 0.16, and 0.20 mm, respectively. * Thickness.

Table 2 shows the results of adhesion force measurements after repeatedly positioning the measurement area with a Multi75Al-G AFM tip (BudgetSensors). Each data point represents the average of 256 measurements of an adhesion force on the chosen CW section (2.04 × 8.15 μm), and the standard deviation is shown as the error bar. Two, five, and four measurements were conducted separately on day D1, day D2, and day D3, respectively. On day D1, the average adhesion forces of the two relocating tests D11 and D12 were 10.6 nN and 10.7 nN, with standard deviations of 1.6 nN and 1.6 nN, respectively. On day D2, the averages and standard deviations (in brackets) of adhesion forces for relocating tests D21, D22, D23, D24, and D25 were 11.1 nN (1.9 nN), 10.8 nN (1.9 nN), 10.7 nN (1.8 nN), 10.6 nN (1.4 nN), and 10.7 nN (1.5 nN), respectively. On day D3, the averages and standard deviations for tests D31, D32, D33, and D34 were 10.8 nN (2.2 nN), 10.8 nN (1.8 nN), 10.7 nN (1.5 nN), and 10.7 nN (1.7 nN), respectively. The absolute value of adhesion force is dependent on the tip type, tip radius, tip force constant, surface roughness, measurement condition (eg in solutions, in the air, or in the dry atmosphere). Therefore, it is expected that different authors have different adhesion force values considering the different test conditions.

Table 2. Repeated adhesion force measurements on day 1 (D1), day 2 (D2), and day 3 (D3).

Day	Test	Average (nN)	SD (nN)[a]	Sample size (pixels)
D1	D11	10.6	1.6	256
	D12	10.7	1.6	256
D2	D21	11.1	1.9	256
	D22	10.8	1.9	256
	D23	10.7	1.8	256
	D24	10.6	1.4	256
	D25	10.7	1.5	256
D3	D31	10.8	2.2	256
	D32	10.8	1.8	256
	D33	10.7	1.5	256
	D34	10.7	1.7	256
P-value		0.090	0.052[b]	

Dij: jth measurement on day i.
[a] Standard deviation.
[b] Based on mean.

An analysis of variance (ANOVA) was performed at an α level of 0.05 to reveal differences between measurements on the same day and different days. Duncan's multiple range test (MRT) assuming homogeneous variances was used as the post hoc test. Levene's test at an α level of 0.05 was used to evaluate the homogeneity of variances between measurements. A null hypothesis stated that both the means and variances between measurements on D1, D2, and D3 were equal.

The MRT analysis (Table 3) showed that except for the second measurement on day 2 (D22), all the other measurements of adhesion forces had equal means. Levene's test showed that all the measurements of adhesion forces had homogenous variances. Therefore, the null hypothesis was accepted that the measurements of adhesion forces on the wood CW with the positioning method had equal means and variances on the

Table 3. Duncan's multiple range test at an α level of 0.05.

Test	D24	D11	D34	D12	D33	D23	D25	D22	D32	D31	D21
Average (nN)	10.6	10.6	10.7	10.7	10.7	10.7	10.7	10.8	10.8	10.8	11.1

Dij: jth measurement on the day i.

same day and different days. It can be concluded that the positioning method has good repeatability regarding the means and the variances of the measurement of adhesion forces on the wood CW.

Table 4 showed the results of repeated adhesion force measurements on the same positioned CW section. Between measurements, the tip was kept on the wood surface and all the measurement conditions were the same. The averages and standard deviations (in brackets) of the five relocating tests were 10.7 nN (1.7 nN), 10.6 nN (1.7 nN), 10.5 nN (1.4 nN), 10.4 nN (1.4 nN), and 10.4 nN (1.3 nN), respectively. ANOVA and Levene's tests at an α level of 0.05 were used to statistically evaluate the data. The P values showed that the means and variances of the measurements were not significantly different. It could be concluded that the AFM device had high repeatability in the adhesion force measurements on the CW. This is important when repeated measurements of a surface before and after treatments are made. The magnitude of the force will be affected if the tip geometry changes (measurements with no treatments will not repeatable), and this may lead to misinterpretation of the results because the error caused by a partially broken tip will skew the data in one direction.

Table 4. Repeated adhesion force measurements on the same positioned cell wall section.

Test	Average (nN)	SD (nN)[a]	Sample size (pixels)
1	10.7	1.7	256
2	10.6	1.7	256
3	10.5	1.4	256
4	10.4	1.4	256
5	10.4	1.3	256
P-value	0.850	0.167[b]	—

[a] Standard deviation.
[b] Based on mean.

Effect of Temperature on the Adhesion Force

We have used the aforementioned positioning method to study the effect of temperature on the adhesion force. These tests were conducted as initial experiments to simulate the environmental effects (in this case, elevated temperatures) and to test if even small changes in an adhesion force could be detected when the spatial surface variability was suppressed (by precise repositioning). Measurements under elevated temperatures were conducted on days D4 and D5 at 60°C and 90°C. As shown in Fig 9, two relocating measurements were carried out at 60°C when the sample was heated for 40 and 70 min, and the average adhesion forces were 10.0 and 10.1 nN, respectively. Student's t-test (two-tail) at an α level of 0.05 showed that there was no significant difference between the two measurements ($P = 0.611$). For the relocating measurements at 100°C, the average adhesion forces were 11.2, 11.0, and 11.4 nN, respectively, when the heating lasted for 40 min, 90 min, and 120 min. An ANOVA at an α level of 0.05 showed that the adhesion forces of the three relocating tests were not significantly different ($P = 0.137$). Thus, the relocating method also had high repeatability when the sample was heated. After the heating was turned off, the sample was stabilized in a desiccator (RH less than 15%, 20 ± 3°C) for 12 h. As shown in Fig 9, after heating tests at 90°C, the adhesion forces increased from around 11 nN to around 13 nN.

The sources of variation in adhesion forces during heating can come from measurement error, cantilever, and the CW structure. As discussed earlier, the positioning method using the natural pit aperture had high repeatability; thus, the measurement error due to relocating the same CW section and device error could be ignored. From room temperature (20 ± 3°C) to the heating temperature (90 ± 0.5°C), the changes in

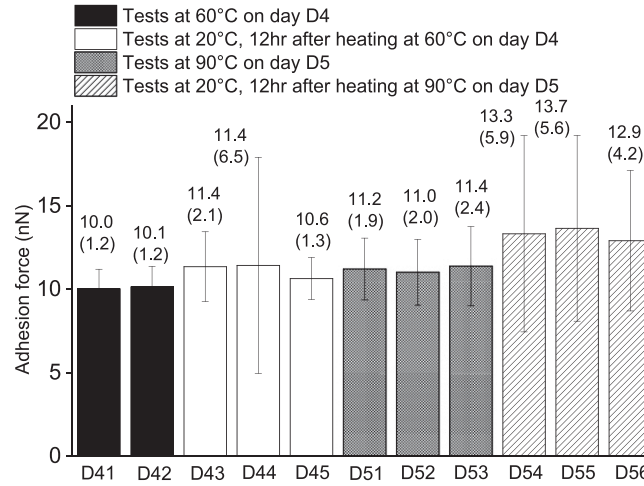

Figure 9. Relocating measurements at elevated temperatures and after 12 h of stabilization. D41 and D42: relocating tests at 60°C on day D4; D43, D44, and D45: relocating tests at 20°C, 12 h after heating tests at 60°C on day D4; D51, D52, and D53: relocating tests at 90°C on day D4; relocating tests at 20°C, 12 h after heating tests at 90°C on day D5. Each data point is the average of 256 measurement points. Error bar: standard deviation. The values of the average and standard deviation (in brackets) of adhesion forces are shown on the top of each column.

the elastic modulus of silicon and geometry dimensions of the cantilever could be ignored because of the low thermal coefficient expansion (Watanabe et al 2004; Shirai 2013; Middelmann et al 2015). The property of the cantilever was viewed as unchanged in the temperature range in this study.

The effect of temperature on adhesion force measurements had been studied on more homogeneous materials, and controversial results were reported. The adhesion force of polystyrene films increased with increasing temperature, which was attributed to the temperature dependence of stiffness and elastic–plastic properties of the sample (Cappella and Stark 2006). In a dry nitrogen atmosphere, the adhesion force between the AFM tip and a grooved silicon surface decreased with increasing temperature, which was explained as a consequence of the broken van der Waal bonds (Lai et al 2015). A decrease in the adhesion forces was also observed between the AFM tip and the cross-linked polydimethylsiloxanes as a function of temperature, and it was ascribed to the decrease in the intermolecular interactions. The wood surface is more complex and challenging for interpretation of the temperature effect on adhesion measurement because of the natural random textures, various roughness, and heterogeneity. The increase in the variances after heating reflects this complexity.

The effect of temperature on wood was widely studied in the literature regarding wood modification with heat treatment and wood-accelerated aging at elevated temperatures. After heat treatment at 240°C in nitrogen for 8 h, the wettability of wood surface by polar solvent was lower with a strong decrease in the acid–base component of the surface free energy and a decrease in the O/C ratio. Higher water contact angles were also reported after the wood sample was treated with vapor at 190 and 212°C (Miklečić and Jirouš-Rajković 2016). After heat treatment below 100°C in nitrogen, the water contact angle of spruce wood experienced almost no changes. However, an abrupt change to 90° happened in the temperature range between 100 and 160°C (Hakkou et al 2005).

The decreasing wettability of the wood surface can be caused by the degradation of hemicelluloses and extractives, which migrate toward the wood surface. Hemicelluloses were reported to

degrade first with the deacetylation process with released acetic acids and the dehydration process with the reduction of hydroxyl groups (Weiland and Guyonnet 2003; Nuopponen et al 2005; Liu et al 2017). The fats and waxes were reported to move to the surface during the heat treatment at 100-160°C and disappeared at elevated temperatures higher than 180°C (Nuopponen et al 2003).

The heat treatment of wood in this study was conducted in the AFM environmental chamber at 60 and 90°C in nitrogen for short durations. Limited chemical changes on the surface could be expected in the mild treatment process, and some extractives might begin to move to the surface. Spruce contains both hydrophilic and lipophilic extractives. The hydrophilic components are mainly lignans (0-2.5 mg/g^{-1}), which are a group of phenolic compounds. The lipophilic components are mainly free fatty acids (1.2-2.8 mg/g^{-1}) and resin acids (0.8-2.4 mg/g^{-1}) (Willför et al 2003).

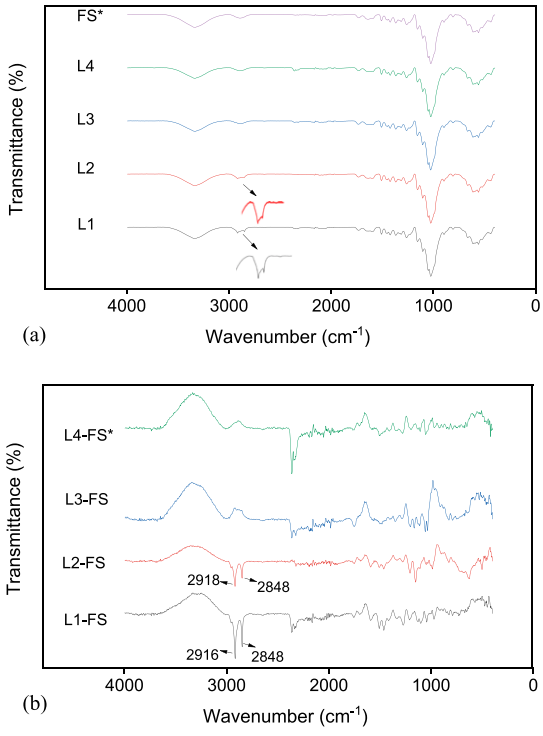

Figure 10. Spectra of the surface layers of treated and fresh wood sample (FS) (a); the difference spectra of surface layers of treated and fresh wood sample (b). L1, L2, L3, and L4 were cut in sequence from the treated sample in the direction perpendicular to the measured surface by atomic force microscopy. * Fresh sample.

FTIR spectra were collected from the surface layers of the wood sample. As shown in Fig 10(a), compared with the fresh sample, no shifts in the main absorption bands were observed in the fingerprint range of 600-1800 cm^{-1} for the four surface layers of the treated wood sample. Compared with the fresh sample, the spectra of the surface layers L1 and L2 in the thermally treated sample showed different peaks in the range of 2900 and 2800 cm^{-1}. The surface layers L3 and L4 did not show these two peaks. Figure 10(b) shows the difference spectra of the surface layers in the treated sample and the fresh sample. The difference spectrum of the treated sample surface L1 and the fresh sample showed two strong sharp peaks at 2918 and 2848 cm^{-1}, respectively. The L2 layer, which was 0.23 mm under the surface L1 layer, also showed the difference in peaks at 2916 and 2848 cm^{-1} with less intensity. The two peaks did not appear in the deeper layers, L3 and L4, which were 0.62 and 0.82 mm away from the surface.

Nuopponen et al (2003) reported that after the wood was treated at temperatures between 100 and 180°C, the difference spectrum showed absorption bands at 2924 and 2855 cm^{-1}, which resulted from the C-H stretching of saturated hydrocarbons. The same author assumed that the movement of the resins along the parenchyma cells began at heating temperatures lower than 90°C, considering that the melting point of softwood resins is between 42 to 90°C. The spectra of the extractives recovered by toluene from the spruce wood showed two strong bands at 2921 and 2851 cm^{-1}, which were attributable to methylene/methyl (Ajuong and Birkinshaw 2004).

The two peaks of 2918 and 2848 cm^{-1} in the difference spectrum on the surface L1 and at 2918 and 2848 cm^{-1} on the layer L2 that we measured confirm the results reported in the literature (Nuopponen et al 2003; Ajuong and Birkinshaw 2004) and indicate that the extractives in the treated

sample moved to the surface during the heating process. The volatile and nonvolatile compounds in the extractives might have contaminated the AFM tip and the wood sample surface, thus causing changes in the measured adhesion forces during and after the heating process.

CONCLUSIONS

In this article, a positioning method using a bordered pit as a natural recognizable feature of the wood surface is presented. The method was demonstrated using experiments under various scenarios ranging from simply repeated positioning without treatments to removal of the specimens, subjecting them to treatments and repositioning the tip again. Turning the device off and on was included in the experiments, and various time delays between measurements were investigated. The positioning method was used to investigate the effect of elevated temperature on the attraction/adhesion force between the silicon tip and wood surface, and the results showed that the proposed positioning method was robust and repeatable. This suppressed the variability because of spatial variation of the surface and allowed for more precise studying of the effects of various treatments on surface properties of wood using the AFM.

ACKNOWLEDGMENTS

The authors gratefully acknowledge the support of the Fraunhofer Wilhelm-Klauditz-Institut (WKI) with the specimen preparation and access to the AFM and FTIR. This research was partially funded by the German Research Foundation (DFG) as a part of the DFG Graduate College GRK2075 at the Technical University in Braunschweig.

REFERENCES

Abu Quba AA, Schaumann GE, Karagulyan M, Diehl D (2020) A new approach for repeated tip-sample relocation for AFM imaging of nano and micro sized particles and cells in liquid environment. Ultramicroscopy 211:112945.

Acda MN, Devera EE, Cabangon RJ, Ramos HJ (2011) Effects of plasma modification on adhesion properties of wood. Int J Adhes Adhes 32:70-75.

Ajuong EMA, Birkinshaw C (2004) The effects of acetylation on the extractives of Sitka Spruce (*Picea sitchensis*) and Larch (*Larix leptoleptis*) wood. Eur J Wood Wood Prod 62(3):189-196.

Arnould O, Arinero R (2015) Towards a better understanding of wood cell wall characterisation with contact resonance atomic force microscopy. Compos. Part A Appl. Sci. Manuf. 74:69–76.

Cappella B, Stark W (2006) Adhesion of amorphous polymers as a function of temperature probed with AFM force-distance curves. J Colloid Interface Sci 296(2):507-514.

Casdorff K, Keplinger T, Burgert I (2017) Nano-mechanical characterization of the wood cell wall by AFM studies: Comparison between AC- and QI™ mode. Plant Methods 13(1):1263.

Domec JC, Lachenbruch B, Meinzer FC (2006) Bordered pit structure and function determine spatial patterns of air-seeding thresholds in xylem of Douglas-fir (*Pseudotsuga menziesii*; Pinaceae) trees. Am J Bot 93(11):1588-1600.

Frybort S, Obersriebnig M, Müller U, Gindl-Altmutter W, Konnerth J (2014) Variability in surface polarity of wood by means of AFM adhesion force mapping. Colloids Surf A Physicochem Eng Asp 457:82-87.

Hakkou M, Pétrissans M, El Bakali I, Gérardin P, Zoulalian A (2005) Wettability changes and mass loss during heat treatment of wood. Holzforschung 59(1):35-37.

Janel S, Werkmeister E, Bongiovanni A, Lafont F, Barois N (2017) CLAFEM: Correlative light atomic force electron microscopy. Methods Cell Biol 140:165-185.

Jin X, Kasal B (2016) Adhesion force mapping on wood by atomic force microscopy: Influence of surface roughness and tip geometry. R Soc Open Sci 3(10):160248.

Kao AP, Connelly JT, Barber AH (2016) 3D nanomechanical evaluations of dermal structures in skin. J Mech Behav Biomed Mater 57:14-23.

Koran Z (1977) Tangential pitting in black spruce tracheid. Wood Sci Technol 11(2):115-123.

Lai T, Chen R, Huang P (2015) Temperature dependence of microscale adhesion force between solid surfaces using an AFM. J Adhes Sci Technol 29(2):133-148.

Liu XY, Timar MC, Varodi AM, Sawyer G (2017) An investigation of accelerated temperature-induced ageing of four wood species: Colour and FTIR. Wood Sci Technol 51(2):357-378.

Liu Z, Li Z, Zhou H, Wei G, Song Y, Wang L (2005) Mechanically engraved mica surface using the atomic force microscope tip facilitates return to a specific sample location. Microsc Res Tech 66(2-3):156-162.

Markiewicz P, Goh MC (1997) Identifying locations on a substrate for the repeated positioning of AFM samples. Ultramicroscopy 68(4):215-221.

Meincken M, Evans PD (2009) Nanoscale characterization of wood photodegradation using atomic force microscopy. Eur J Wood Wood Prod 67(2):229-231.

Meincken M, Evans PD (2010) Use of atomic force microscopy to detect wavelength dependent changes in wood

veneers, and spin coated lignin and cellulose films exposed to solar radiation. Int Wood Prod J 1(2):75-80.

Middelmann T, Walkov A, Bartl G, Schödel R (2015) Thermal expansion coefficient of single-crystal silicon from 7 K to 293 K. Phys Rev B Condens Matter Mater Phys 92(17):13.

Miklečić J, Jirouš-Rajković V (2016) Influence of thermal modification on surface properties and chemical composition of beech wood (*Fagus sylvatica L.*). Drv Ind 67(1): 65-71.

Nguyen HK, Prevosto D, Labardi M, Capaccioli S, Lucchesi M, Rolla P (2011) Effect of confinement on structural relaxation in ultrathin polymer films investigated by local dielectric spectroscopy. Macromolecules 44(16):6588-6593.

Nowicki M, Richter A, Wolf B, Kaczmarek H (2003) Nanoscale mechanical properties of polymers irradiated by UV. Polymer (Guildf) 44(21):6599-6606.

Nuopponen M, Vuorinen T, Jms S, Viitaniemi P (2003) The effects of a heat treatment on the behaviour of extractives in softwood studied by FTIR spectroscopic methods. Wood Sci Technol 37(2):109-115.

Nuopponen M, Vuorinen T, Jämsä S, Viitaniemi P (2005) Thermal modifications in softwood studied by FT-IR and UV resonance Raman spectroscopies. J Wood Chem Technol 24(1):13-26.

O'Hagan BMG, Doyle P, Allen JM, Sutton K, McKerr G (2004) The effects of atomic force microscopy upon nominated living cells. Ultramicroscopy 102(1):1-5.

Proff C, Abolhassani S, Dadras MM, Lemaignan C (2010) In situ oxidation of zirconium binary alloys by environmental SEM and analysis by AFM, FIB, and TEM. J Nucl Mater 404(2):97-108.

Revilla RI, Guan L, Zhu XY, Quan BG, Yang YL, Wang C (2012) Electrowetting phenomenon on nanostructured surfaces studied by using atomic force microscopy. J Phys Chem C 116(27):14311-14317.

Robertson C, Wertheimer MR, Fournier D, Lamarre L (1996) Study on the morphology of XLPE power cable by means of atomic force microscopy. IEEE T Dielect El In 3(2): 283–288.

Shirai K (2013) Temperature dependence of Young's Modulus of silicon. Jpn J Appl Phys 52(8R):88002.

Sikora A (2013) Development and utilization of the nanomarkers for precise AFM tip positioning in the investigation of the surface morphology change. Appl Opt 43:163-171.

Sikora A (2014) Improvement of the scanning area positioning repeatability using nanomarkers developed with a nanoscratching method. Meas Sci Technol 25(5): 55401.

Sirviö J, Kärenlampi P (1998) Pits as natural irregularities in softwood fibers. Wood Fiber Sci 30(1):27-39.

Stamm AJ (1970) Maximum effective pit pore radii of the heartwood and sapwood of six softwoods as affected by drying and resoaking. Wood Fiber Sci 1(4): 263-269.

Su M, Pan Z, Dravid VP (2004) A convenient and rapid sample repositioning approach for atomic force microscopy. J Microscopy 216(Pt 2):194-196.

Watanabe H, Yamada N, Okaji M (2004) Linear thermal expansion coefficient of silicon from 293 to 1000 K. Int J Thermophys 25(1):221-236.

Weiland JJ, Guyonnet R (2003) Study of chemical modifications and fungi degradation of thermally modified wood using DRIFT spectroscopy. Eur J Wood Wood Prod 61(3): 216-220.

Willför S, Hemming J, Reunanen M, Eckerman C, Holmbom B (2003) Lignans and lipophilic extractives in norway spruce knots and stemwood. Holzforschung 57(1):27-36.

Wu A, Li Z, Yu L, Wang H, Wang E (2002) A relocated technique of atomic force microscopy (AFM) samples and its application in molecular biology. Ultramicroscopy 92(3-4):201-207.